Accepted Manuscript

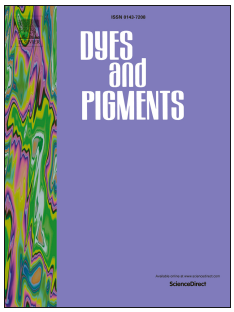

A dual-functional chemosensor for fluorescent on-off and ratiometric detection of Cu^{2+} and Hg^{2+} and its application in cell imaging

Shuang Zeng, Shi-Jie Li, Xue-Jiao Sun, Ting-Ting Liu, Zhi-Yong Xing

PII: S0143-7208(19)30884-8

DOI: https://doi.org/10.1016/j.dyepig.2019.107642

Article Number: 107642

Reference: DYPI 107642

To appear in: *Dyes and Pigments*

Received Date: 20 April 2019

Revised Date: 4 May 2019

Accepted Date: 13 June 2019

Please cite this article as: Zeng S, Li S-J, Sun X-J, Liu T-T, Xing Z-Y, A dual-functional chemosensor for fluorescent on-off and ratiometric detection of Cu^{2+} and Hg^{2+} and its application in cell imaging, *Dyes and Pigments* (2019), doi: https://doi.org/10.1016/j.dyepig.2019.107642.

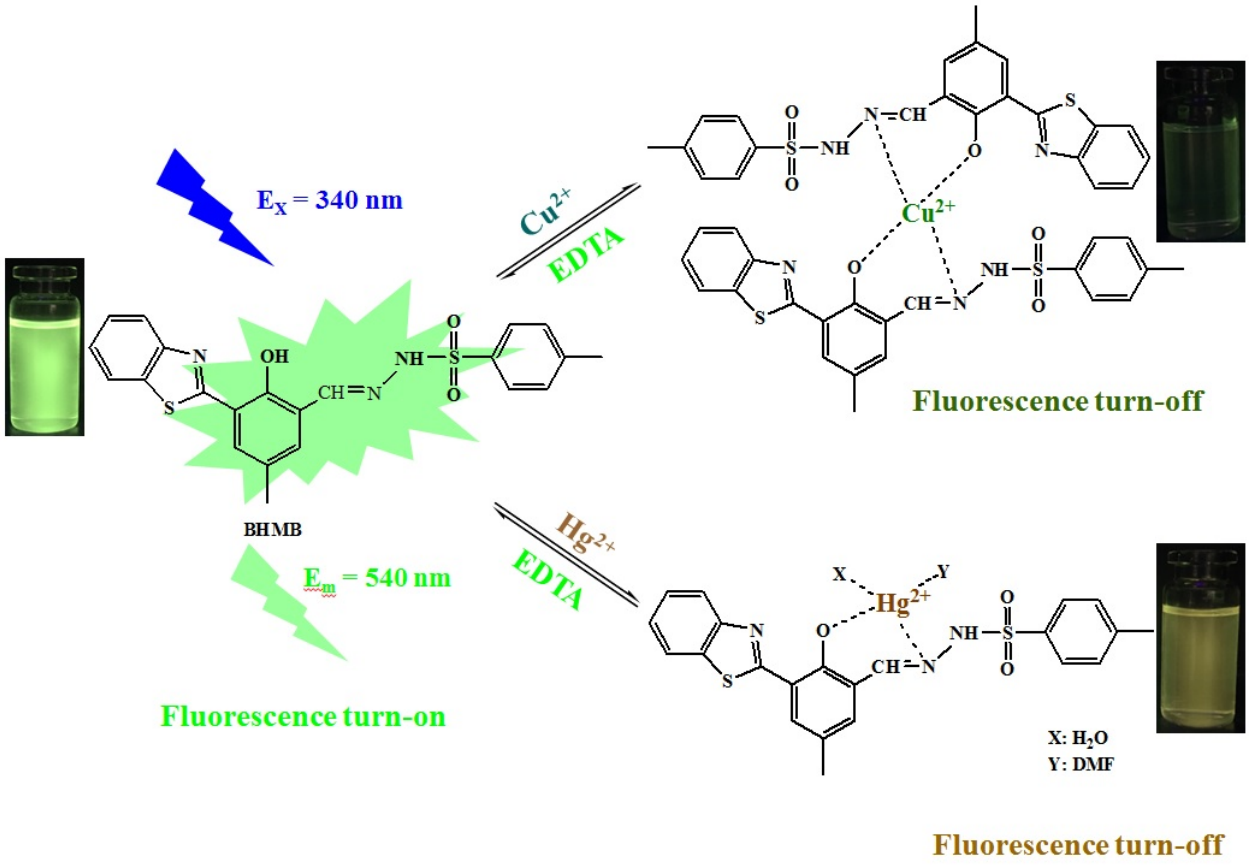

A dual-functional chemosensor for fluorescent on-off and ratiometric detection of Cu^{2+} and Hg^{2+} and its application in cell imaging

Shuang Zeng [a, 1], Shi-Jie Li [b, 1], Xue-Jiao Sun [a], Ting-Ting Liu [a], Zhi-Yong Xing [a,*]

[a] Department of Applied Chemistry, College of Science, Northeast Agricultural University, Harbin 150030, PR China

[b] College of Life Science, Northeast Agricultural University, Harbin 150030, PR China

* Corresponding author at: Department of Applied Chemistry, College of Science, Northeast Agricultural University, Harbin 150030, PR China

E-mail addresses: zyxing@neau.edu.cn, Tel: +86 451 5519 1810, Fax: +86 451 5519 0317

[1] These authors contributed equally to this work and should be considered co-first authors.

Abstract: A dual-functional chemosensor **BHMB** was synthesized and characterized. It showed highly selectivity through significant fluorescence turn-off and obvious color change towards Cu^{2+} and Hg^{2+}, respectively. The binding ratios of **BHMB** to Cu^{2+} and Hg^{2+} confirmed by job' plot were 2:1 and 1:1, respectively. Moreover, the detection of limit of **BHMB** to Cu^{2+} and Hg^{2+} was confirmed as 4.47×10^{-8} M and 6.72×10^{-7} M, respectively. Especially, **BHMB** was successfully used in test paper for fast identification of Cu^{2+} and Hg^{2+}, logic gate construction and cell imaging in human stromal cell (HSC).

Key Words: benzothiazole; Cu^{2+}; Hg^{2+}; ratiometric chemosensor; cell imaging

1. Introduction

The issue of heavy metals pollution, especially mercury pollution, which is a fatal hazard to our environment and human health, has been a hot topic on its qualitative and quantitative analysis. As is well known, Hg^{2+} is easily accumulate in human body and the profound toxicity lies in its high binding ability with thiols and amino groups in proteins and enzymes, which may further induce some diseases such as kidney failure, motor disorders and tumor formation [1-4]. On the other hand, Cu^{2+}, the third most abundant and necessary trace element in the human body, plays a closely associate with biological processes including cellular respiration, connective tissue development and bone formation [5-8]. However, either deficiency or overloading of Cu^{2+} will increase the risk of a number of diseases such as heart disease, iron-deficient anemia, Alzheimer's, Parkinson's, Menkes and Wilson's diseases, metabolic disorders and cancer [9-13]. According to the requirement of Environmental Protection Agency (U.S. EPA), the maximum permitted limits of the Hg^{2+} and Cu^{2+} ion in drinking water are less than 2 ppb (2 ng/L) and 1.3 ppm (1.3 mg/L), respectively. Hence, it is of great importance for the development of efficient method for monitoring of Hg^{2+} and Cu^{2+} in the water sources and biological environments.

Fluorescence-based probes, which display a lot of virtues such as high sensitivity and selectivity, rapid response and simplicity for heavy and transition metal ions in environmental and biological detection, had received considerable attention among researchers on its development [14, 15]. Many fluorescent probes were developed for the detection of Hg^{2+} [16-22] or Cu^{2+} [23-29], but most of them were one probe for one analyte. Recently, the designing idea that one probe for muti-target had gained more and more researchers' interesting due to its high efficiency and cost reduction. Although a lot of multifunctional probes were successfully developed for

simultaneous detection of various analytes [30-38], only a few of them were of qualitative and quantitative analysis for Hg^{2+} and Cu^{2+} simultaneously based on different fluorophores such as rhodamine [39, 40], benzothiazole [41], pyrene [42], dansyl [43, 44], BODIPY [45], and ferrocenyl–naphthalimide [46]. So, it is still full of demand to develop muti-functional chemosensors for the detection of Hg^{2+} and Cu^{2+}.

2-(2'-Hydroxyphenyl) benzothiazole (HBT), an excellent fluorophore basing the excited state intramolecular proton transfer (ESIPT) mechanism, is usually employed in construction chemosensors due to its excellent properties in the fields of photophysics and photochemistry [41, 47]. Herein, we designed and synthesized HBT-based chemosensor **BHMB** through condensation of 3-(benzo[d]thiazol-2-yl)-2-hydroxy-5-methylbenzaldehyde and 4-methylbenzenesulfono-hydrazide. Chemosensor **BHMB** displayed high selectivity to Hg^{2+} and Cu^{2+} through different signal response in DMF-H_2O (3/7, v/v, 0.01M HEPES, pH=7.0) medium. Moreover, the application of **BHMB** in real samples, logic gate construction and cell imaging were all investigated.

2. Experimental

2.1. Materials and instruments

All chemicals were analytical or spectroscopic grade which were obtained commercially and used without further purification. All metal ion solutions were prepared by its perchlorate or nitrate salts. Buffer solution was prepared by hydroxyethyl piperazine ethanesulfonic acid (HEPES) and NaOH.

Melting point was recorded on a Beijing XT4-100X microscopic melting point apparatus. FT-IR spectra were measured by SEWERE ALPHA-T (Bruker Company, DEU). ^{1}H NMR spectra

and ^{13}C NMR spectra were recorded on a Bruck AV-600 spectrometer using DMSO-d_6 as the solvent. The model of PHS-3C meter (Shanghai, China) was used for the pH measurement. Absorption spectra were recorded on a Shimadzu UV-2700 UV–vis spectrometer at 25 ℃. Fluorescence measurements were measured on a Perkin Elmer LS55 fluorescence spectrometer. Mass spectra were determined on a Waters Xevo UPLC/G2-SQ Tof MS spectrometer.

2.2. Synthesis

Compounds 1-2 were prepared according to our previous reported procedure [47].

2.2.1 Synthesis of Sensor **BHMB**

Compound **2** (102 mg, 0.38 mmol) and 4-Methylbenzenesulphonyl hydrazide (73 mg, 0.39 mmol) were dissolved in ethanol (10 mL), and the mixture was refluxed 6 h. After the complete consumption of the starting material monitored by TLC, the mixture was cooled to room temperature. After which was poured into water (20 mL), the solid was collected by filtration and washed 3 times with distilled water and dried to give **BHMB**. Yield: 82.4%. m.p.:231-233 °C. ^{1}H NMR (600 MHz, DMSO-d6) (Fig. S1) δ (ppm) 12.43 (s, 1H), 11.77 (s, 1H), 8.29 (s, 1H), 8.17 (d, J = 7.8 Hz, 1H), 8.07 (d, J = 8.0 Hz, 1H), 7.90 (s, 1H), 7.80 (d, J = 8.2 Hz, 2H), 7.57 (t, J = 7.6 Hz, 1H), 7.51(s, 1H), 7.48 (t, J = 7.8 Hz, 1H) 7.45 (d, J = 8.4 Hz, 2H), 2.37 (s, 3H), 2.33 (s, 3H). ^{13}C NMR (151 MHz, DMSO-d_6) (Fig. S2) δ (ppm) 166.23, 153.81, 151.56, 145.43, 144.23, 136.37, 134.00, 131.29, 130.95, 130.34, 129.43, 127.59, 127.29, 126.10, 122.69, 122.62, 120.93, 118.61, 21.48, 20.39. HRMS (m/z) (TOF MS ES^+) (Fig. S3): calcd for $C_{22}H_{19}N_3O_3S_2$: 438.0946 $[M+H]^+$, found: 438.0933.

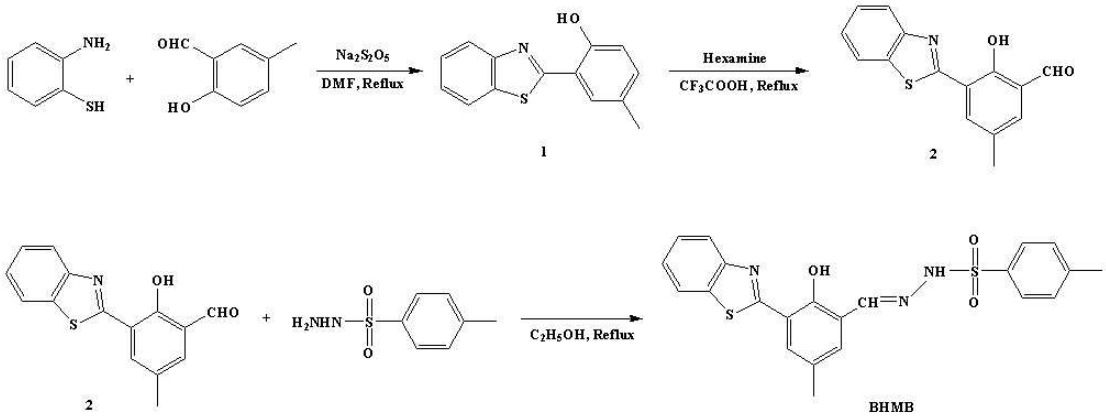

Scheme 1. Synthesis of chemosensor **BHMB**.

2.2. General information

The stock solution of **BHMB** (0.1 mM) was prepared in DMF. The stock solutions (10 mM) of the cationic salts including Na^{+}, K^{+}, Mg^{2+}, Ca^{2+}, Ba^{2+}, Cr^{3+}, Mn^{2+}, Fe^{2+}, Fe^{3+}, Co^{2+}, Ni^{2+}, Cu^{2+}, Ag^{+}, Zn^{2+}, Cd^{2+}, Hg^{2+}, Al^{3+} and Pb^{2+} were prepared with ultrapure water, respectively. The test solution were prepared by adding appropriate stock solution of **BHMB** (0.1 mM) and DMF using pipette and diluted with HEPES buffer (10 mM) for the measurement of UV-vis absorption and fluorescence spectra. The excitation was set at 340 nm for the measurement of fluorescence, and the excitation and emission slit widths were set at 5 nm and 10 nm, respectively.

2.3. Preparation of [**BHMB**-Cu^{2+}] and [**BHMB**-Hg^{2+}]

The compound **BHMB** (10 mg, 0.023 mmol) and $Cu(ClO_4)_2 \cdot 6H_2O$ (17..2 mg, 0.046 mmol) or $HgCl_2$ (6.3 mg, 0.023 mmol) were dissolved in ethanol (10 mL), respectively. Then the mixture was refluxed under stirring. After the consumption of **BHMB** monitored by TLC, the mixture was cooled to room temperature. Then the complexes were obtained by removing the solvent under reduced pressure.

2.4. Cell culture and staining

Human stromal cell line (HSC), a fibroblast cell line which was purchased from ATCC

(CRL-4003), has been used to evaluate whether **BHMB** could detect Cu^{2+} in cells. HSC were routinely cultured in mixture medium (DMEM:F-12=1:1), which was supplemented with 10% heat-inactivated FBS, 100 U/mL penicillin, and 100 μg/mL streptomycin at 37 □, 5% CO_2. HSC were planted into 6-well plates with sterile cover glass at concentration of 10^5 cells/well. After 48 hours, the media contained Cu^{2+} at concentration of 0, 10 and 100 μM and without FBS was used to incubate cells 2 hours for chemical treatment. Then fibroblast cells were fixed by using a standard paraformaldehyde fixation protocol and were rinsed with DMF: H_2O = 3:7 mixture solutions. Then cells were stained with **BHMB** (10 μM) for 2 hours. Lastly, the cover glass were mounted over slide glass with anti-fluorescence quenching agent and imaged by fluorescence microscope.

3. Results and Discussion

*3.1. Spectrum studies of **BHMB** with different metal ions*

The UV-visible absorbance of chemosensor **BHMB** were firstly measured upon addition of different metal ions (Na^+, K^+, Ag^+, Mg^{2+}, Ba^{2+}, Ni^{2+}, Ca^{2+}, Mn^{2+}, Fe^{2+}, Co^{2+}, Cu^{2+}, Zn^{2+}, Hg^{2+}, Cd^{2+}, Pb^{2+}, Fe^{3+}, Cr^{3+} and Al^{3+}) in the solution of DMF-H_2O (3/7, v/v, 0.01M HEPES, pH = 7.0) (Fig. 1a), the result showed that the addition of Cu^{2+} caused a significant change in which the absorbance of **BHMB** centered at 365 nm disappeared while a new peak at 434 nm formed. As for the addition of Hg^{2+}, which caused the absorbance spectrum of **BHMB** centered at 365 nm changed broader and the maximum absorbance peak slightly took red-shift to 376 nm. The above phenomenon indicated that the interaction of **BHMB** with Cu^{2+}/Hg^{2+} occurred and further enhanced the degree of conjugation of **BHMB**-Cu^{2+}/Hg^{2+} system which caused the red-shift of absorbance spectrum of **BHMB**. Moreover, the fluorescence spectrums of **BHMB** before and after

addition of above-mentioned metal ions were measured, respectively (Fig. 1b). **BHMB** itself displayed the strong fluorescence centered at 540 nm which was attributed by the keto emission generated from the excited-state intramolecular proton transferred process [41] illustrated in Fig. S4. However, the addition of tested metal ions to the solution of **BHMB** showed that Hg^{2+}, especially the Cu^{2+} completely quenched the fluorescence of **BHMB.** This result might attributed to co-contribution effect of the heavy atom effect of Cu^{2+}/Hg^{2+} and the inhibition of ESIPT process after coordination of phenolic hydroxyl group with Cu^{2+}/Hg^{2+} that previously reported by other researchers [37, 48, 49], and also indicated the existence of interaction between the chemosensor **BHMB** and Cu^{2+}/Hg^{2+}.

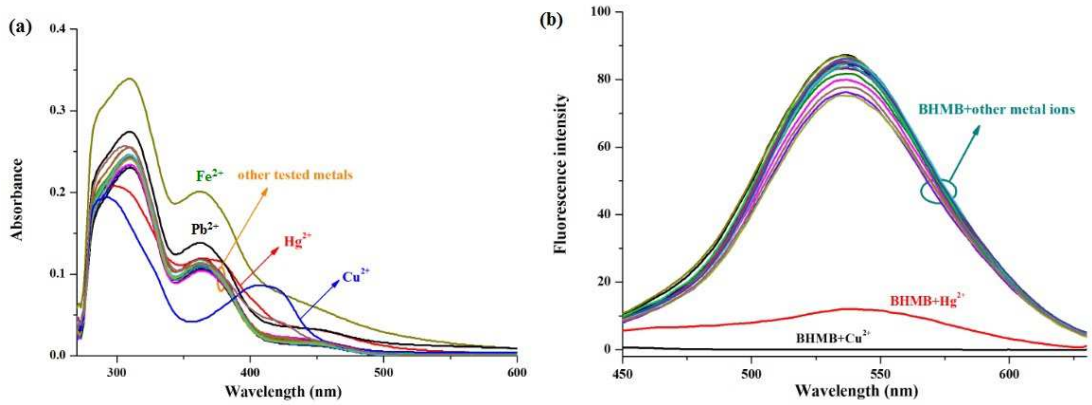

Fig.1 (a) Absorption spectra of **BHMB** (10 μM) recorded without and with different metals (5.0 equiv.) in DMF-H_2O (3/7, v/v, 0.01M HEPES, pH=7.0). (b) Fluorescence spectra of **BHMB** (10 μM) without and with different metals (5.0 equiv.) in DMF-H_2O (3/7, v/v, 0.01M HEPES, pH=7.0).

In order to investigated the detailed variation of **BHMB** upon the addition of different equivalent Cu^{2+}/Hg^{2+}, the UV-visible and fluorescence titration of **BHMB** were measured, respectively. Upon gradual addition of Cu^{2+}, the absorbance centered at 365 nm of **BHMB** was decreased and meanwhile absorbance centered at 434 nm was increased (Fig. 2a), a clear isobestic point at 388 nm was formed, all of these indicating the complex formation of **BHMB** with Cu^{2+}. The good relationship between the absorbance intensity ratio (A_{434}/A_{365}) versus the concentration of Cu^{2+} (0-5 μM) was detected (Fig. S5), which indicated that **BHMB** could be used as a

ratiometric chemosensor for the detection of Cu^{2+}. The limit of detection was calculated as 4.47×10^{-8} M (according to the 3σ/k, where σ is the standard deviation of the blank measurements, and k is the slope of the intensity ratio versus sample concentration plot) [41, 50]. With regarding to the addition of Hg^{2+} to the solution of **BHMB** (Fig. 2b), absorbance at 311 nm was decreased gradually and a slight red-shift from 365 nm to 375 nm was found with an isobestic point at 372 nm, all these results indicated the happens of interaction between **BHMB** and Hg^{2+}. The LOD was determined as 6.72×10^{-7} M according to the good linear relationship between the absorbance intensity at 311 nm and the concentration of Hg^{2+} (0-5 μM) using above mentioned method (Fig. S6).

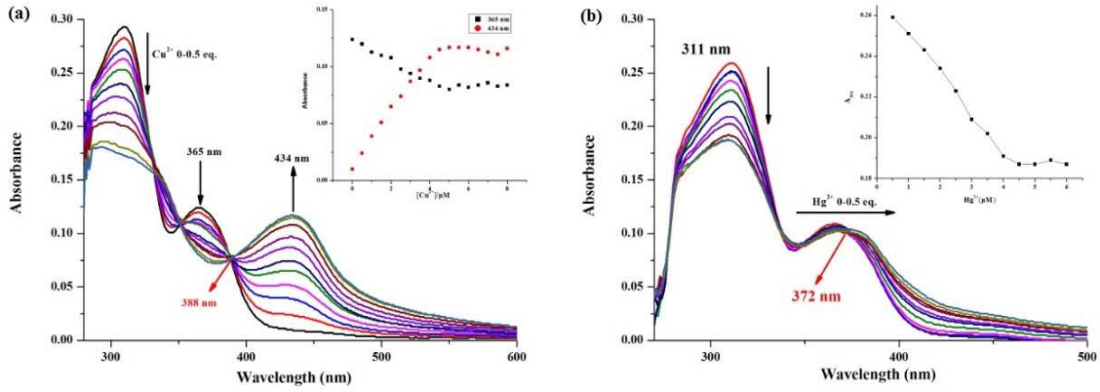

Fig. 2 (a) Absorption titration of **BHMB** (10 μM) upon addition of Cu^{2+} (0-0.5 equiv.) in DMF-H_2O (3/7, v/v, 0.01M HEPES, pH = 7.0), Insert: plot of absorbance intensity at 365 nm and 434 nm of **BHMB** versus Cu^{2+} (0-5.0 equiv.) ; (b) Absorption titration of **BHMB** (10 μM) upon addition of Hg^{2+} (0-0.5 equiv.) in DMF-H_2O (3/7, v/v, 0.01M HEPES, pH = 7.0), Insert: plot of absorbance intensity at 311 nm of **BHMB** versus Hg^{2+} (0-0.5 equiv.).

On the other hand, fluorescence titrations of **BHMB** to Cu^{2+}/Hg^{2+} were depicted in Fig. 3, and the results showed that the fluorescence intensity of **BHMB** was gradually decreased whatever the addition of metal ions was Cu^{2+} or Hg^{2+}. Moreover, the addition of Cu^{2+} and Hg^{2+} induced the color of **BHMB** solution changed from bright green to dark green and khaki, respectively. This result made it possible to distinguish Cu^{2+} and Hg^{2+}, and further realized the dual function of **BHMB** to detect Cu^{2+} and Hg^{2+}. According to the recorded fluorescence intensity

of **BHMB** with the added amount of Cu^{2+} and Hg^{2+}, it could be found that the fluorescence intensity of **BHMB** almost reached a platform when the amount of Cu^{2+} and Hg^{2+} added was 5 μM and 10 μM, respectively. This result indicated the binding ratio of **BHMB** to Cu^{2+} and Hg^{2+} was 2:1 and 1:1, respectively. The detection limit of **BHMB** to Cu^{2+} and Hg^{2+} was determined as 8.14×10^{-8} M (Fig. S7) and 1.29×10^{-7} M (Fig. S8), respectively.

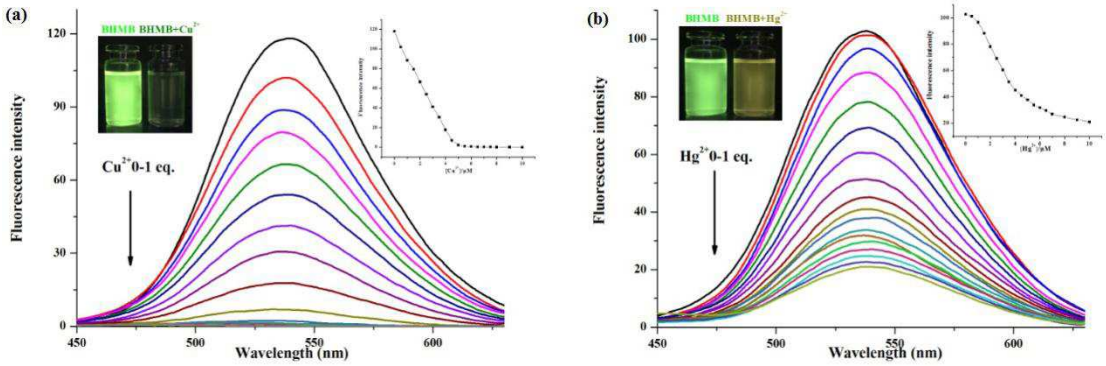

Fig. 3 (a) Fluorescence titration of **BHMB** (10 μM) upon addition of Cu^{2+} (0-1.0 equiv.) in DMF-H_2O (3/7, v/v, 0.01M HEPES, pH = 7.0), Insert: plot of fluorescence intensity at 540 nm of **BHMB** versus Cu^{2+} (0-0.5 equiv.) and color change, E_x = 340 nm; (b) Fluorescence titration of **BHMB** (10 μM) upon addition of Hg^{2+} (0-1.0 equiv.) in DMF-H_2O (3/7, v/v, 0.01M HEPES, pH = 7.0), Insert: plot of fluorescence intensity at 540 nm of **BHMB** versus Hg^{2+} (0-0.5 equiv.) and color change, λ_{ex} = 340 nm.

Furthermore, in order to verify the resistance ability of interference which might come from other co-existence metal ions, competition experiments of **BHMB** to Cu^{2+} and Hg^{2+} were carried out by adding other tested metal ions (Fig. 4) , respectively. The results showed that **BHMB** had high selectivity to Cu^{2+}/ Hg^{2+} without disturbance of tested metal ion and could be competent for the qualitative detection of Cu^{2+}/ Hg^{2+} in relative complex surroundings.

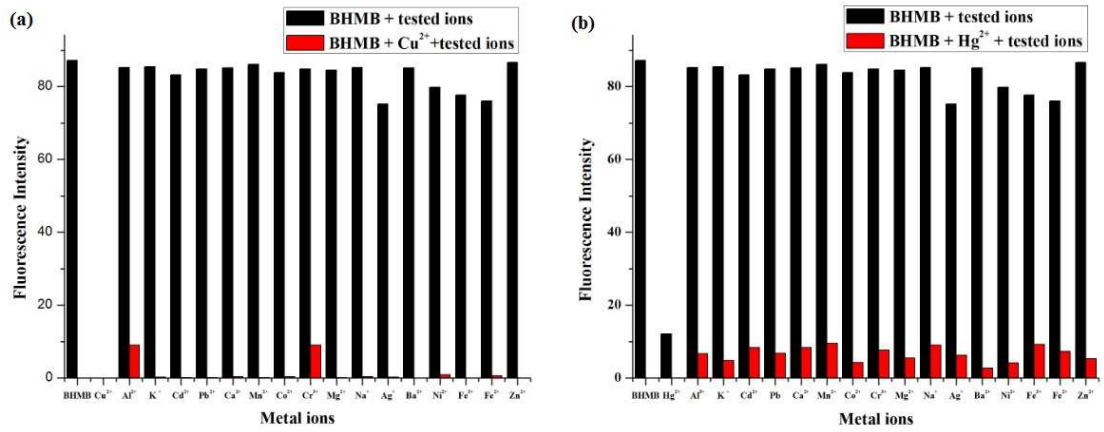

Fig. 4 Competition experiments of **BHMB** toward Cu^{2+} (a) and Hg^{2+} (b) in the presence of 5 equiv. of other metal cations. [**BHMB**]=10 μM, [Cu^{2+}]=50 μM, [Hg^{2+}]= 50 μM, and [X^{n+}]=50 μM in DMF/H_2O (3/7, v/v, 0.01M HEPES, pH = 7.0). λ_{ex} = 340 nm.

*3.2. pH profiles of compound **BHMB***

In order to evaluate the practical applicability of **BHMB**, the compatible pH range for the detection of Cu^{2+} and Hg^{2+} were determined by fluorescence spectrum, respectively. As shown in Fig.5, chemosensor **BHMB** itself showed lower fluorescence intensity (recorded at λ_{em}=540 nm) at pH range of 2-5, while it significantly increased when the pH value was more than 5, and then the fluorescence intensity was almost kept constant in the range of pH 7-13, showing excellent stability of chemosensor **BHMB** in the wide range from neutral to alkaline environment. Upon the addition of Cu^{2+}, the fluorescence intensity was almost same as that of **BHMB** itself in the range of pH = 2-4. Interestingly, a significant distinction in fluorescence intensity of pH ranging from 6 to 13, especially in the range of pH = 7-9 (Fig. 5a). This result showed that **BHMB** was an excellent candidate probe for the detection of Cu^{2+} in biological applications. On the other hand, the fluorescence intensity of **BHMB**-Hg^{2+} system was recorded in different pH medium (Fig. 5b). The result showed that the optimum condition for the detection of Hg^{2+} was pH = 7-8, which was also adequate for Hg^{2+} detection in biological surrounding.

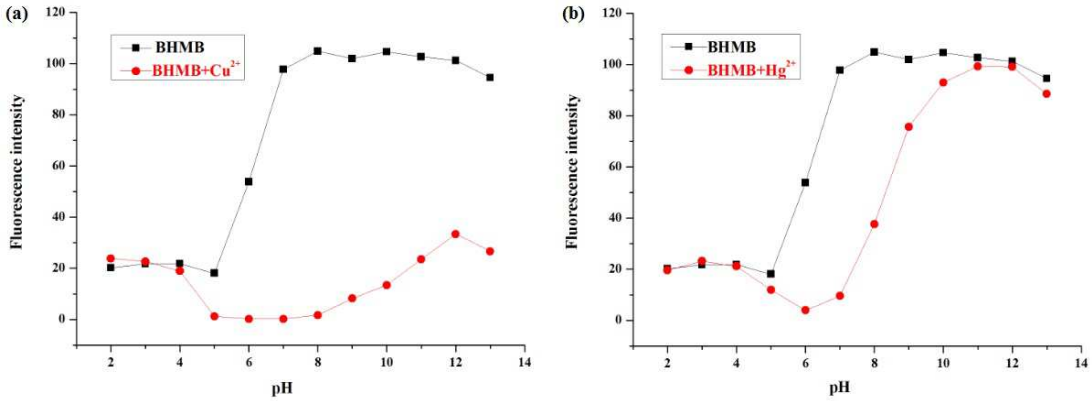

Fig. 5 (a) Plot showing the influence of **BHMB** (10 μM) in the absence and prescence of Cu^{2+} in DMF/H_2O (3/7, v/v) at different pH medium; (b) Plot showing the influence of **BHMB** (10 μM) in the absence and presence of Hg^{2+} in DMF/H_2O (3/7, v/v) at different pH medium.

3.3. Binding stoichiometry and sensing mechanism

The binding ratio of **BHMB** to Cu^{2+} and Hg^{2+} were further determined by job'plot (Fig. 6), respectively. The fitting results were illustrated in Fig. 6, and 2:1 and 1:1 stoichiometry were calculated for **BHMB** bonding to Cu^{2+} and Hg^{2+}, respectively. The ESI-MS spectrum of **BHMB**-Cu^{2+} (Fig. 7) showed peaks at 460.0755, 897.1677 and 958.0756 were assigned to the [**BHMB** + Na^+]$^+$, [2**BHMB** + Na^+]$^+$ and [2(**BHMB** - H^+) +Cu^{2+} + Na^+]$^+$, respectively. Moreover, peaks at 533.1292, 606.1688 and 729.1266 of complex of **BHMB**-Hg^{2+} depicted in Fig. 7, were attributed to [**BHMB** + DMF + Na^+]$^+$, [**BHMB** + 2DMF + Na^+]$^+$, and [**BHMB** - H^+ +Hg^{2+} + DMF + H_2O]$^+$, respectively. According to the Benesi-Hilderbrand plot, the association constants of **BHMB** to Cu^{2+} and Hg^{2+} were counted to be 3.42×10^2 $M^{-1/2}$ and 5.11×10^4 M^{-1}, respectively (Fig. S9-S12).

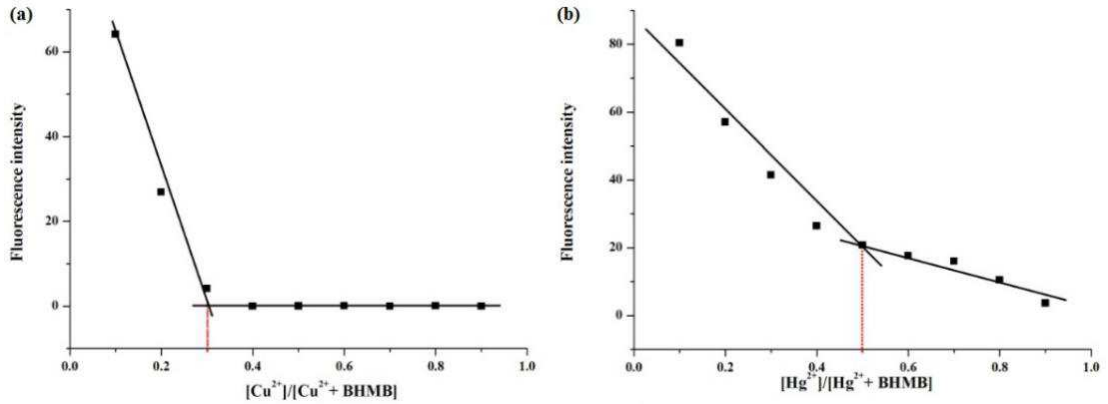

Fig. 6. Job plot of **BHMB**-X^{n+} complex formation. {[X^{n+}]/([X^{n+}]+ [**BHMB**])} is the molar fraction of X^{n+} ion. (a) $X^{n+} = Cu^{2+}$; (b) $X^{n+} = Hg^{2+}$.

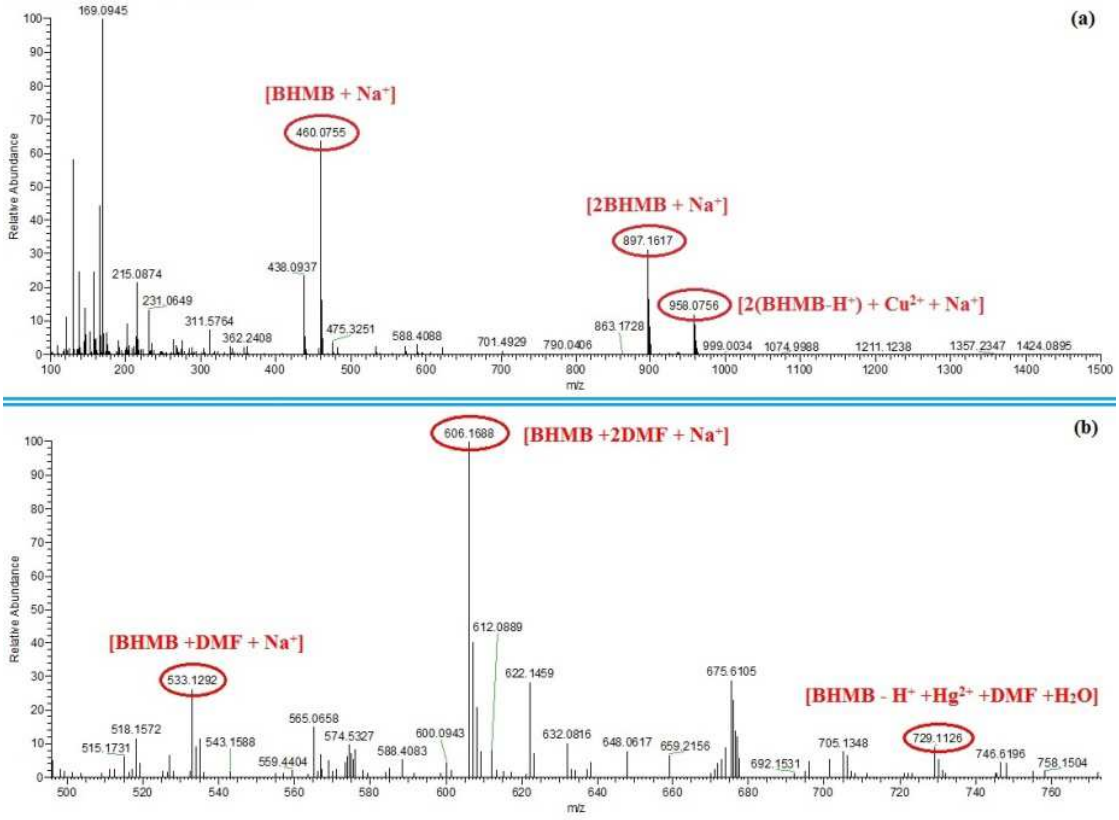

Fig. 7. ESI–MS spectrum of **BHMB** (10 μM) upon addition of Cu^{2+} (a) and Hg^{2+} (b) in DMF.

In order to investigate the binding mode of **BHMB** to Cu^{2+}/Hg^{2+}, the FT-IR spectrum of **BHMB** in the absence and presence of Cu^{2+}/Hg^{2+} were measured, respectively. As for the chemosensor **BHMB** itself, these peaks at 1094 cm^{-1}, 1605 cm^{-1}, 3049 cm^{-1}, 3221 cm^{-1}, were attributed to the stretching vibration of S=O, C=N, N-H and O-H, respectively. Upon the addition

of Cu^{2+} into the solution of compound **BHMB** (Fig. S13), the characteristic absorbance peaks of -OH and -NH were broadened and shifted to 3506 cm^{-1} and 3147 cm^{-1}, respectively. Moreover, the characteristic frequency of the imine C=N band increased from 1605 cm^{-1} to 1612 cm^{-1}. These obvious changes indicated that the hydroxyl oxygen atom and the imine nitrogen atom were involved in the coordination with Cu^{2+} ion. While the addition of Hg^{2+} into the solution of **BHMB** (Fig. S14), the correspondence characteristic frequency mentioned above including S=O, C=N, N-H and O-H were all decreased and shifted to 1093 cm^{-1} 1597 cm^{-1}, 3104 cm^{-1} and 3183 cm^{-1}, respectively. This suggested that compound **BHMB** might interact with Hg^{2+} ions through the hydroxyl oxygen atom and the imine nitrogen atom.

To further investigate the binding site of **BHMB with** Cu^{2+} and Hg^{2+}, ^{1}HNMR titrations were carried out (Fig. 8), respectively. The obvious change was that the proton signal of hydroxyl O-H was gradually decreased upon the addition of Cu^{2+} (Fig. 8a). Moreover, the similar phenomenon was found in that of addition of Hg^{2+} (Fig. 8b). These results strongly indicated the deprotonation of phenolic hydroxyl group upon the interaction with Cu^{2+} or Hg^{2+}, which also further confirmed the inhibition of ESIPT process and resulted in the fluorescence quenching of **BHMB** mentioned above.

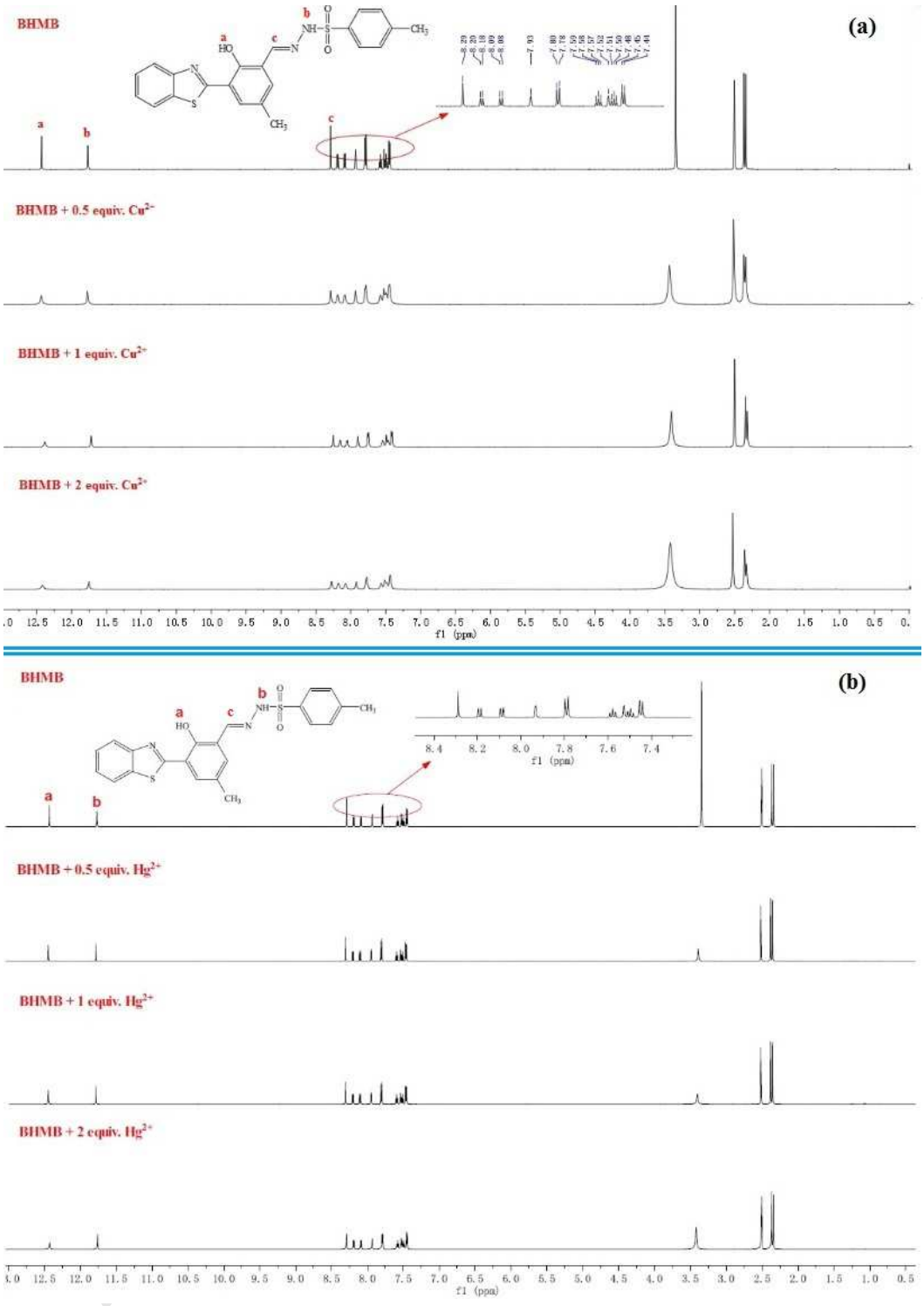

Fig. 8 ^{1}H NMR spectra of **BHMB** with Cu^{2+} (a) and Hg^{2+} (b) in DMSO-d_6.

Taking above experimental results including job' plot, HRMS, FT-IR and ^{1}HNMR titration, the possible mechanism of the interaction of **BHMB** with Cu^{2+} and Hg^{2+} were illustrated in Scheme 2.

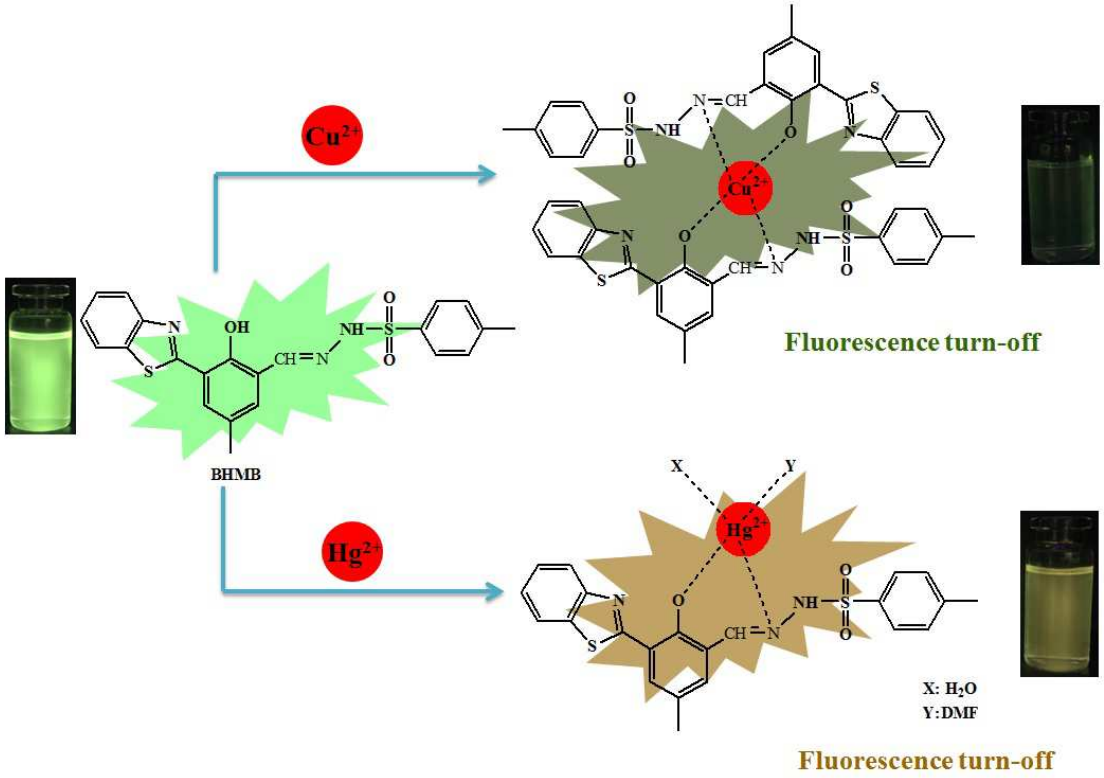

Scheme 2 Possible interaction mechanism of **BHMB** with Cu^{2+} and Hg^{2+}

3.4. Reversibility studies

Reversibility was a key factor to evaluate a chemosensor in practical application such as logic gate construction. As shown in Fig. 9, the alternate addition of Cu^{2+} (Fig. 9a) or Hg^{2+} (Fig. 9b) and EDTA to the solution of **BHMB** resulted in the variation in fluorescence intensity and color. Although emission signal decay to some extent could be found for several cycles, the **BHMB**-based colorimetric chemosensor showed good stability. This result indicated that the strong stability of complex of **BHMB**-Cu^{2+}/Hg^{2+}, and could be used in the construction of logic gate through different output signals upon adding different materials.

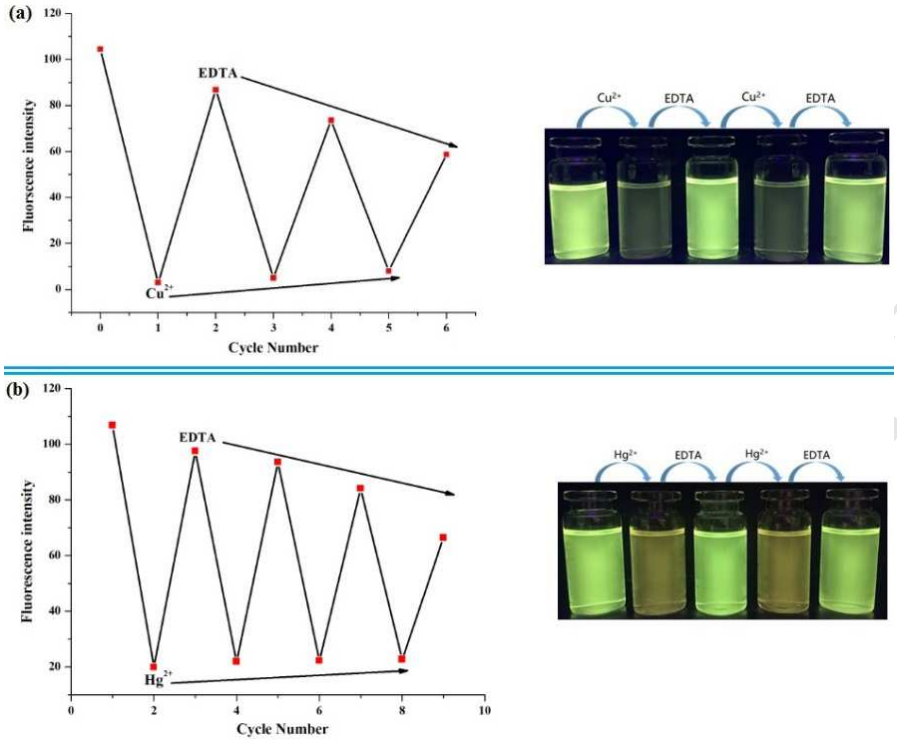

Fig. 9 (a) Reversible changes in color and fluorescence intensity of BHMB (10 μM) at 540 nm in DMF/H_2O (3/7, v/v, 0.01M HEPES, pH = 7.0) upon alternate addition of Cu^{2+} and EDTA; (b) Reversible changes in color and fluorescence intensity of **BHMB** (10 μM) at 540 nm in DMF/H_2O (3/7, v/v, 0.01M HEPES, pH = 7.0) upon alternate addition of Hg^{2+} and EDTA.

4. Applications

4.1 Real sample detection

In order to investigate the applicability of the probe **BHMB** to the detection of Cu^{2+} and Hg^{2+} in real water samples. We collected samples from the tap water in the Department of Chemistry and the Songhua River in Harbin, and Cu^{2+} or Hg^{2+} with different concentrations (0, 1, 2, 3, 4 and 5 μM) were added to these corresponding water samples. The fluorescence responses of Probe **BHMB** at 540 nm in those real water samples were determined, respectively. As shown in Fig. 10, we found that the detection of Cu^{2+} (Fig. 10a) or Hg^{2+} (Fig. 10b) in real water samples was similar to the results detected in ultrapure water (Fig. S7-S8). In addition, the good linear relationships (Fig. S15-S18) were found in real water samples, which were all consistent with the linear relationship previously obtained in ultrapure water. These results showed that the probe **BHMB**

had high recovery and precision for the detection of Cu^{2+} and Hg^{2+} in real water samples, and also indicated that it could be applied in the analysis of Cu^{2+} and Hg^{2+} in environmental water samples.

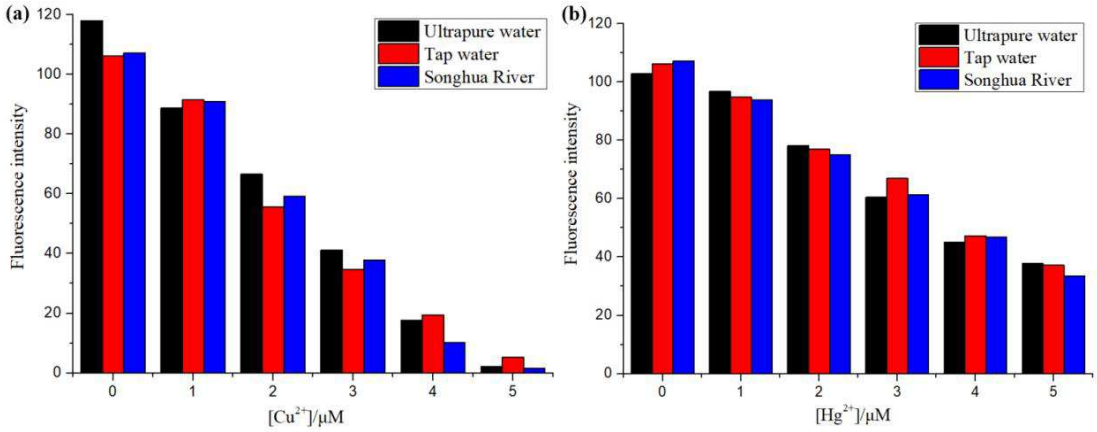

Fig. 10 Fluorescent detection of BHMB (10 μM) in "ultrapure water", "tap water", and "Songhua River" upon addition of different concentration of (a) Cu^{2+} and (b) Hg^{2+}, respectively. The data was obtained at 540 nm.

4.2 Application in test paper

Due to the good selectivity of the probe **BHMB** for Cu^{2+} and Hg^{2+} with the significant fluorescence color change for detection, the test strip experiments of the probe **BHMB** for Cu^{2+} and Hg^{2+} were examined, respectively. As shown in Fig. 11, with the increased concentration of Cu^{2+} (Fig. 11a) or Hg^{2+} (Fig. 11b), test papers (top and bottom) displayed a visible color change from initial yellow to final bluish violet under 365 nm UV light, but the transitional colors of **BHMB** with different concentration of Cu^{2+} was not same as that of Hg^{2+}, which was another method to differentiate between Cu^{2+} and Hg^{2+}. The result also indicated that the probe **BHMB** could be applied to the fast detection of Cu^{2+} and Hg^{2+} by test strip.

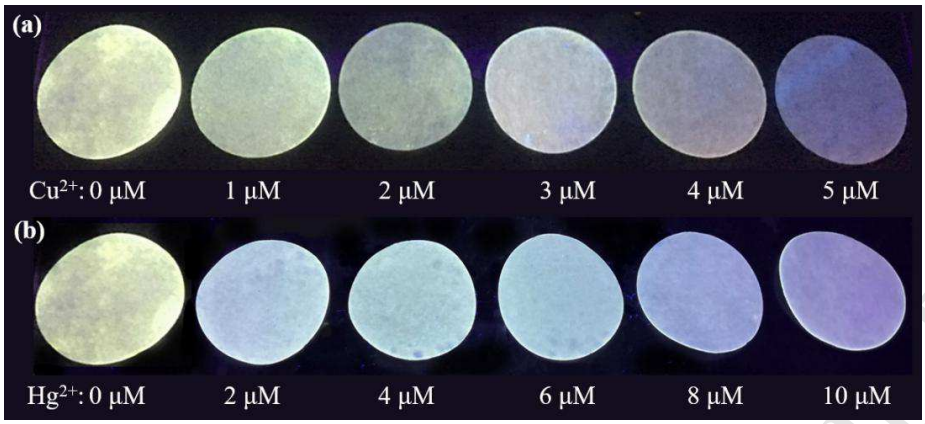

Fig. 11 The photographs of probe BHMB on test strips with different concentrations of (a) Cu^{2+} and (b) Hg^{2+} at room temperature under 365 nm UV light, respectively.

4.3 Logic gate construction

Thanks to the fluorescence quenching-restoration cycle of probe **BHMB** (10 μM) with Cu^{2+} (10 μM) or Hg^{2+} (10 μM) and EDTA (10 μM) (Fig. 12a, b), one logic gate can be implemented on Boolean logic operations, which is a **IMPLICATION** logic gate and displaying memory unit with two inputs (In 1 and In 2) and one output(Fig. 12c, d). We set Cu^{2+} or Hg^{2+} and EDTA separately as inputs In 1 and inputs In 2, whose presence and absence were itemized as 1 and 0. The output signal is emission intensity at 540 nm and the threshold value is considered as 40 au. When the fluorescence intensity is higher than the threshold value, the output signal is On (1). And when the fluorescence intensity is lower than the threshold value, the output signal is Off (0). Based on the above basic logic gates, when the Cu^{2+} or Hg^{2+} and EDTA were all presence or absence, the output signal is On (1). When inputs 1 and 2 were in a (1, 0) state, the output signal is Off (0). In addition, in order to achieve reversible cyclic operation of logic gates, we further installed the memory storage device to the logic circuit. When the output signal in a Off (0) state, the input signal can be reset by the memory unit to return the output to the On (1) state. Thus, this logic circuit with memory element can cause the entire process to be repeated several times.

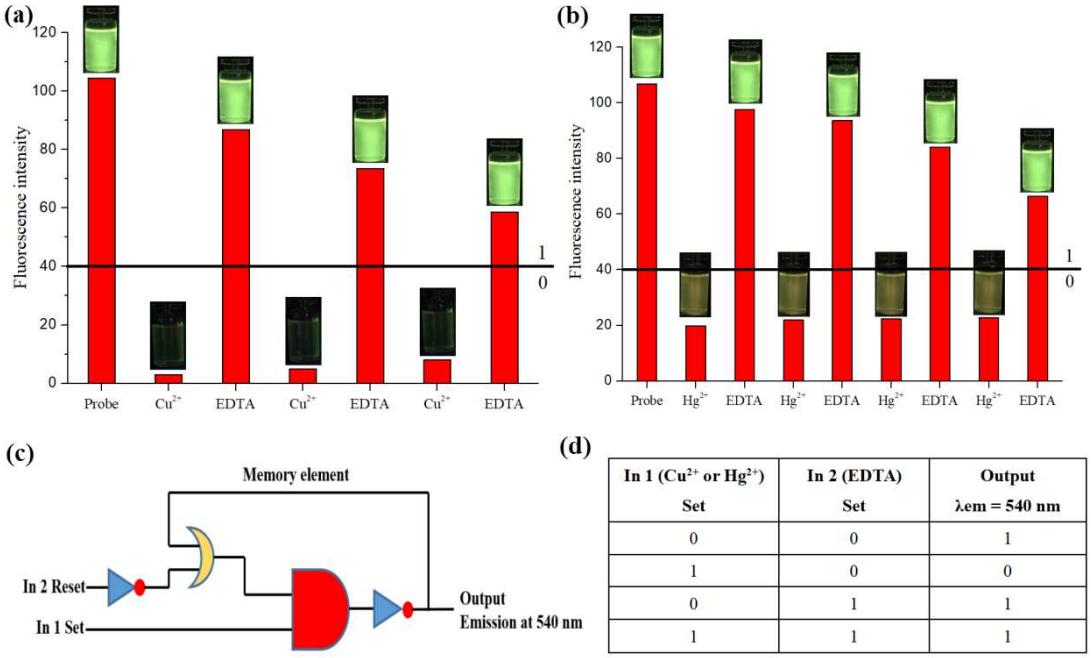

In 1 (Cu^{2+} or Hg^{2+}) Set	In 2 (EDTA) Set	Output λem = 540 nm
0	0	1
1	0	0
0	1	1
1	1	1

Fig. 12 (a) bar diagram represents input (In 1 = Cu^{2+} and In 2= EDTA) and output emissions (at 40 au); (b) bar diagram represents input (In 1 = Hg^{2+} and In 2= EDTA) and output emissions (at 40 au); (c) IMPLICATION logic gate with two inputs (In 1 and In 2) and one output; (d) corresponding truth table.

4.4 cell imaging

To further investigate the practical applicability of probe **BHMB** in biological systems, the cells imaging experiments were measured by fluorescence microscope. Compared to the complex of **BHMB**-Hg^{2+}, the complex of **BHMB**-Cu^{2+} has almost no fluorescence emission and can exist in a wide pH range. Thus, we used the human stromal cells (HSC) that was incubated different amounts of Cu^{2+} and 10 μM of **BHMB**. As shown in Fig. 13a, when the cells was incubated 2 h with **BHMB** (10 μM), the aquamarine fluorescence was observed under fluorescent microscope. With increased concentration of Cu^{2+}, the fluorescence intensity is gradually weakens and finally quenched when 100 μM of Cu^{2+} was incubated with cells (Fig. 13b, c). This result indicates that the probe **BHMB** can be used to track Cu^{2+} in biological systems.

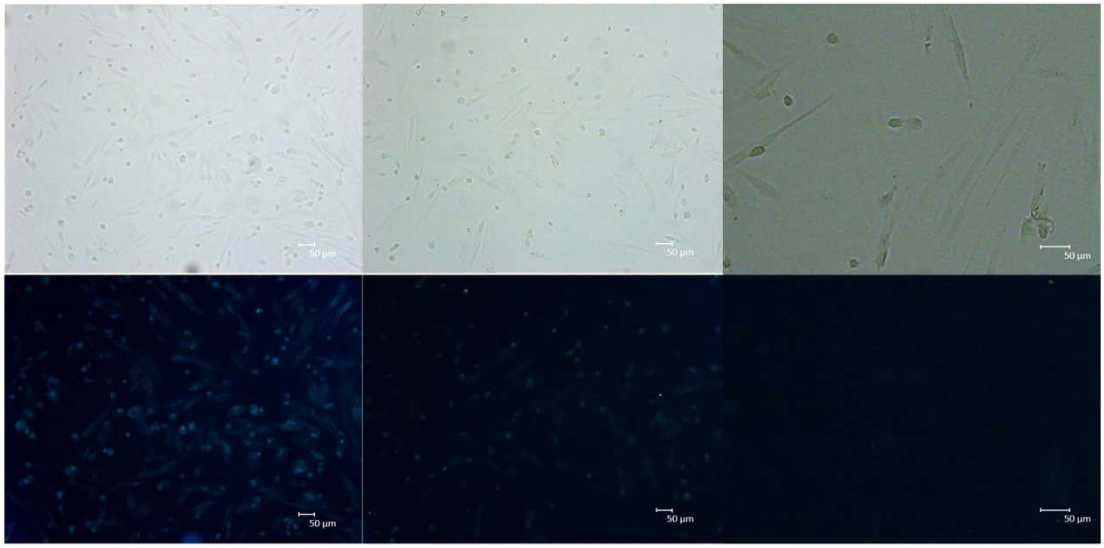

(a) BHMB 10 μM **(b) BHMB +Cu^{2+}(10 μM)** **(c) BHMB +Cu^{2+}(100 μM)**

Fig. 13 (a) The cells was incubated 2 h with **BHMB** (10 μM); (b) cells was incubated 10 μM of Cu^{2+} and 10 μM of **BHMB**; (c) cells was incubated 100 μM of Cu^{2+} and 10 μM of **BHMB**.

Conclusions

In conclusion, a dual-functional chemosensor **BHMB** was synthesized and characterized. It showed high selectivity to Hg^{2+} and Cu^{2+} through significant fluorescence turn-off and obvious color change towards Cu^{2+} and Hg^{2+} in DMF-H_2O (3/7, v/v, 0.01M HEPES, pH=7.0) medium, respectively. The binding ratios of **BHMB** to Cu^{2+} and Hg^{2+} were determined as 2:1 and 1:1, respectively. Moreover, the detection of limit of **BHMB** to Cu^{2+} and Hg^{2+} was confirmed as 4.47×10^{-8} M and 6.72×10^{-7} M, respectively. Especially, **BHMB** was successfully used in test paper for fast identification of Cu^{2+} and Hg^{2+}, logic gate construction and cell imaging in human stromal cell (HSC).

Acknowledgements

This work was supported by the Postdoctoral Scientific Research Developmental Fund of Heilongjiang Province (No. LBH-Q14023). We would like to thank Professor Jinlong Li (Qiqihar University) for NMR and ESI-mass running.

Appendix A. Supplementary data

Supplementary data to this article can be found online at

References

[1] Nolan EM, Lippard SJ. Tools and tactics for the optical detection of mercuric ion. Chem Rev 2008; 108: 3443-80.

[2] Carter KP, Young AM, Palmer AE. Fluorescent Sensors for Measuring Metal Ions in Living Systems. Chem Rev 2014; 114: 4564-601.

[3] Kaura B, Kaur N, Kumar S. Colorimetric metal ion sensors-A comprehensive review of the years 2011–2016. Coord Chem Rev 2018; 358: 13-69.

[4] Guo Z, Park S, Yoon J, Shin I. Recent progress in the development of near-infrared fluorescent probes for bioimaging applications. Chem Soc Rev 2014; 43: 16-29.

[5] Cotruvo JA, Aron AT, Ramos-Torres KM, Chang CJ. Synthetic fluorescent probes for studying copper in biological systems. Chem Soc Rev 2015; 44: 4400-14.

[6] Que EL, Domaille DW, Chang CJ. Metals in Neurobiology: Probing Their Chemistry and Biology with Molecular Imaging. Chem Rev 2008; 108: 1517-49.

[7] Uauy R, Olivares M, Gonzalez M. Essentiality of copper in humans. Am J Clin Nutr 1998; 67: 952S-9S.

[8] Araya M, Olivares M, Pizarro F. Copper in human health. Int J Environ Health 2007; 1: 608-20.

[9] Gaetke LM, Chow CK. Copper toxicity, oxidative stress, and antioxidant nutrients. Toxicology 2003; 189: 147-63.

[10] Strausak D, Mercer JF, Dieter HH, Stremmel W, Multhaup G. Copper in disorders with neurological symptoms: Alzheimer's, Menkes, and Wilson diseases. Brain Res Bull 2001; 55: 175-85.

[11] Gaggelli E, Kozlowski H, Valensin D, Valensin G. Copper homeostasis and neurodegenerative disorders (Alzheimer's, prion, and Parkinson's diseases and amyotrophic lateral sclerosis). Chem Rev 2006; 106: 1995-2044.

[12] Santini C, Pellei M, Gandin V, Porchia M, Tisato F, Marzano C. Advances in Copper Complexes as Anticancer Agents. Chem Rev 2014; 114: 815-62.

[13] Millhauser G. Copper binding in the prion protein. Acc Chem Res 2004; 37: 79-85.

[14] Liu HW, Chen L, Xu C, Li Z, Zhang H, Zhang XB, Tan W. Recent progresses in small-molecule enzymatic fluorescent probes for cancer imaging. Chem Soc Rev 2018; 47: 7140-80.

[15] Niu LY, Chen YZ, Zheng HR, Wu LZ, Tung CH, Yang QZ. Design strategies of fluorescent probes for selective detection among biothiols. Chem Soc Rev 2015; 44: 6143-60.

[16] Yuan X, Leng TH, Guo ZQ, Wang CY, Li JZ, Yang WW, Zhu WH. A FRET-based dual-channel turn-on fluorescence probe for the detection of Hg^{2+} in living cells. Dyes Pigm 2019; 161: 403-10.

[17] Kumar A, Chae PS. Fluorescence tunable thiophene-bis(benzimidazole)-based probes for a cascade trace detection of Hg^{2+} and lysine: A molecular switch mimic. Sens. Actuators B Chem 2019; 281: 933-44.

[18] Gupta S, Milton MD. Synthesis of novel AIEE active pyridopyrazines and their applications as chromogenic and fluorogenic probes for Hg^{2+} detection in aqueous media. New J Chem 2018; 42: 2838-49.

[19] Xu J, Li H, Chen Y, Yang B, Jiao Q, Yang Y, Zhu HL. A novel fluorescent probe for Hg^{2+} detection in a wide pH range and its application in living cell imaging. Anal Methods 2018; 10: 5554-8.

[20] Pan SL, Li K, Li LL, Li MY, Shi L, Liu YH, Yu XQ. A reaction-based ratiometric fluorescent sensor for the detection of Hg(II) ions in both cells and bacteria. Chem Commun 2018; 54: 4955-8.

[21] Li CY, Xu F, Li YF, Zhou K, Zhou Y. A fluorescent chemosensor for Hg^{2+} based on naphthalimide derivative by fluorescence enhancement in aqueous solution. Anal Chim Acta 2012; 717: 122-6.

[22] Li Dan, Li CY, Li YF, Li Z, Xu F. Rhodamine-based chemodosimeter for fluorescent determination of Hg^{2+} in 100% aqueous solution and in living cells. Anal Chim Acta 2016; 934: 218-5.

[23] Wu YS, Li CY, Li YF, Li D, Li Z. Development of a simple pyrene-based ratiometric fluorescentchemosensor for copper ion in living cells. Sens. Actuators B Chem 2016; 222: 1226–32.

[24] Jiao X, Xiao Z, Hui P, Liu C, Wang Q, Qiu X, He S, Zeng X, Zhao L. A highly selective and pH-tolerance fluorescent probe for Cu^{2+} based on a novel carbazole-rhodamine hybrid dye. Dyes Pigm 2019; 160: 633-40.

[25] Kumar R, Bawa R, Gahlyan P, Dalela M, Jindal K, Jha PK, Tomar M, Gupta V. Pyrene appended bis-triazolylated 1,4-dihydropyridine as a selective fluorogenic sensor for Cu^{2+}. Dyes Pigm 2019; 161: 162-71.

[26] Liu Y, Wu Y, Guo X, Wen Y, Yang H. Rapid and selective detection of trace Cu^{2+} by

accumulation- reaction-based Raman spectroscopy. Sens Actuators B Chem 2019; 283: 278-83.

[27] Mani KS, Rajamanikandan R, Murugesapandian B, Shankar R, Sivaraman G, Ilanchelian M, Rajendran SP. Coumarin based hydrazone as an ICT-based fluorescence chemosensor for the detection of Cu^{2+} ions and the application in HeLa cells. Spectrochim Acta A Mol Biomol Spectrosc 2019; 214: 170-6.

[28] Ghorai A, Mondal J, Manna AK, Chowdhury S, Patra GK. A novel pyrene based highly selective reversible fluorescent-colorimetric sensor for the rapid detection of Cu^{2+} ions: application in bio-imaging. Anal. Methods 2018; 10: 1063-73.

[29] He C, Zhou H, Yang N, Niu N, Hussain E, Li Y, Yu C. A turn-on fluorescent BOPHY probe for Cu^{2+} ion detection. New J Chem 2018; 42: 2520-5.

[30] Gharami S, Aich K, Patra L, Mondal TK. Detection and discrimination of Zn^{2+} and Hg^{2+} using a single molecular fluorescent probe. New J Chem 2018; 42: 8646-52.

[31] Liu H, Cui S, Shi F, Pu S. A diarylethene based multi-functional sensor for fluorescent detection of Cd^{2+} and colorimetric detection of Cu^{2+}. Dyes Pigm 2019; 161: 34-43.

[32] Erdemir S, Malkondu S. Dual-emissive fluorescent probe based on phenolphthalein appended diaminomaleonitrile for Al^{3+} and the colorimetric recognition of Cu^{2+}. Dyes Pigm 2019; 163: 330-6

[33] Li JZ, Leng TH, Wang ZQ, Zhou L, Gong XQ, Shen YJ, Wang CY. A large Stokes shift, sequential, colorimetric fluorescent probe for sensing Cu^{2+}/S^{2-} and its applications. J Photochem Photobiol A: Chem 2019; 373: 146-53.

[34] Kim MS, Jo TG, Yang M, Han J, Lim MH, Kim C. A fluorescent and colorimetric Schiff

base chemosensor for the detection of Zn^{2+} and Cu^{2+}: Application in live cell imaging and colorimetric test kit. Spectrochim Acta A Mol Biomol Spectrosc 2019; 211: 34-43.

[35] Zhang M, Gong L, Sun C, Li W, Chang Z, Qi D. A newfluorescent-colorimetric chemosensor based on a Schiff base for detecting Cr^{3+}, Cu^{2+}, Fe^{3+} and Al^{3+} ions. Spectrochim Acta A Mol Biomol Spectrosc 2019; 214: 7-13.

[36] Hu Y, Li QQ, Li H, Guo QN, Lu YG, Li ZY. A novel class of Cd(II), Hg(II) turn-on and Cu(II), Zn(II) turn-off Schiff base fluorescent probes. Dalton Trans 2010; 39: 11344-52.

[37] Pannipara M, Al-Sehemi AG, Irfan A, Assiri M, Kalam A, Al-Ammari YS. AIE active multianalyte fluorescent probe for the detection of Cu^{2+}, Ni^{2+} and Hg^{2+} ions. Spectrochim Acta A Mol Biomol Spectrosc 2018; 201: 54-60.

[38] Li NN, Ma YQ, Sun XJ, Li MQ, Zeng S, Xing ZY, Li JL. A dual-function probe based on naphthalene for fluorescent turn-on recognition of Cu^{2+} and colorimetric detection of Fe^{3+} in neat H_2O. Spectrochim Acta A Mol Biomol Spectrosc 2019; 210: 266-74.

[39] Li G, Bai L, Tao F, Deng A, Wang L. A dual chemosensor for Cu^{2+} and Hg^{2+} based on a rhodamine-terminated water-soluble polymer in 100% aqueous solution. Analyst 2018; 143: 5395-403.

[40] Bayindir S. A simple rhodanine-based fluorescent sensor for mercury and copper: The recognition of Hg^{2+} in aqueous solution, and Hg^{2+}/Cu^{2+} in organic solvent. J Photochem Photobiol A: Chem 2019; 372: 235-44.

[41] Gu B, Huang L, Su W, Duan X, Li H, Yao S. A benzothiazole-based fluorescent probe for distinguishing and bioimaging of Hg^{2+} and Cu^{2+}. Analytica Chimica Acta 2017; 954: 97-104.

[42] Puangsamlee T, Tachapermpon Y, Kammalun P, Sukrat K, Wainiphithapong C, Sirirak J,

Wanichacheva N. Solvent control bifunctional fluorescence probe for selective detection of Cu^{2+} and Hg^{2+} via the excimer of pyrenylacetamide subunits. J Lumin 2018; 196: 227-35.

[43] Sie YW, Li CL, Wan CF, Yan H, Wu AT. A novel fluorescence sensor for dual sensing of Hg^{2+} and Cu^{2+} ions. J Photochem Photobiol A: Chem 2018; 353: 19-25.

[44] Pang X, Gao L, Feng H, Li X, Kong J, Li L. A peptide-based multifunctional fluorescent probe for Cu^{2+}, Hg^{2+} and biothiols. New J Chem 2018; 42: 15770-7.

[45] Huang Y, Li CF, Shi WJ, Tan HY, He ZZ, Zheng L, Liu F, Yan J.W. A near-infrared BODIPY-based fluorescent probe for ratiometric and discriminative detection of Hg^{2+} and Cu^{2+} ions in living cells. Talanta 2019; 198: 390-7.

[46] Dong J, Hu J, Baigude H, Zhang H. A novel ferrocenyl–naphthalimide as a multichannel probe for the detection of Cu(II) and Hg(II) in aqueous media and living cells. Dalton Trans 2018; 47: 314-22.

[47] Zeng S, Li SJ, Sun XJ, Li MQ, Xing ZY, Li JL. A benzothiazole-based chemosensor for significant fluorescent turn-on and ratiometric detection of Al^{3+} and its application in cell imaging. Inorg Chim Acta 2019; 486: 654-62.

[48] Al-Sehemi AG, Pannipara M, Kalam A. Quinazolinone derivative: Model compound for determination of dipole moment, solvatochromism and metal ion sensing. Spectrochim Acta A Mol Biomol Spectrosc 2017; 171: 97-103.

[49] Goswami S, Manna A, Mondal M, Sarkar D. Cascade reaction-based rapid and ratiometric detection of H_2S/S^{2-} in the presence of bio-thiols with live cell imaging: demasking of ESIPT approach. RSC Adv 2014; 4: 62639-43.

[50] Zeng S, Li SJ, Sun XJ, Li MQ, Ma YQ, Xing ZY, Li JL. A naphthalene-quinoline based

chemosensor for fluorescent “turn-on” and absorbance-ratiometric detection of Al^{3+} and its application in cells imaging. Spectrochim Acta A Mol Biomol Spectrosc 2018; 205: 276-86.

Highlights

- Chemosensor **BHMB** with benzothiazole fluorophore was synthesized and characterized.
- Chemosensor **BHMB** exhibits highly selective fluorescence responses to Hg^{2+} and Cu^{2+} with significant fluorescence turn-off and color change.
- The limit of detection (LOD) for Cu^{2+} and Hg^{2+} was reached the level of 10^{-8} M and 10^{-7} M, respectively.
- **BHMB** was successfully applied in the detection of Cu^{2+} and Hg^{2+} in test paper and cell imaging in HSC.